New Approach for the T-stress Estimation for Specimens with a U-notch

M. Hadj Meliani [1], Z. Azari[1], G. Pluvinage[1] and Yu.G. Matvienko[2]

[1] Laboratoire de Fiabilité Mécanique, LFM-ENIM, île de saulcy 57045, Université Paul Verlaine de Metz, France. E-mail : hadjmeliani@univ-metz.fr
[2]Mechanical Engineering Research Institute of the Russian Academy of Sciences, 4 M. Kharitonievsky Per., 101990 Moscow, Russia. E-mail: matvienko7@yahoo.com

ABSTRACT. *The concept of the T-stress as a constraint factor has been extended to notch tip stress distribution. The effective T-stress (T_{ef}) has been estimated as the average value of the T-stress in the fracture process zone. The notch fracture toughness $K_{\rho,c}$ has been determined using the Volumetric Method. Transferability is then proposed as a $K_{\rho,c} - T_{ef,c}$ curve and established from 4 specimen types (CT, SENT, DCB and RT) made from X52 pipe steel. Crack stabilisation and crack bifurcation for fracture emanating from notches according to the value of $T_{ef,c}$ is discussed.*

INTRODUCTION

The concept of brittle crack extension resistance is based on the assumption that stress intensity factor dominance exists at a crack-tip. Then, in a region surrounding the crack tip the stress fields can be characterized by the asymptotic mathematical solution [1]

$$\sigma_{ij} = \frac{K_I}{\sqrt{2\pi r}} f_{ij}(\theta) + T\delta_{xi}\delta_{xj} + A_3\sqrt{2\pi r} + 0(r) \qquad (1)$$

where K_I is the stress intensity factor, $f_{ij}(\theta)$ is the angular function, δ_{ij} is the symbol of Kronecker's determinant. A polar coordinate system (r,θ) with an origin at the crack tip is used. The second term is called the *T*-stress. The value of T_{xx}, or simply *T,* is constant stresses acting parallel to the crack line in the direction *xx* with a magnitude proportional to the gross stress in the vicinity of the crack. The third term A_3 is sometimes used as a transferability parameter like the T-stress. The non-singular term *T* represents a tension (or compression) stress. Positive *T*-stress strengthens the level of crack tip stress triaxiality and leads to high crack-tip constraint while negative *T*-stress leads to the lost of constraint.

The following facts characterise the T-stress and its effects:

a) The value of T is sensitive to loading mode, specimen geometry, specimen and crack sizes. For example, according to Eisele et al 2] and Matvienko [3], the T-stress increases from high negative value to low negative or positive values when specimen loading mode and geometry change from tension to bending.

b) Sherry et al [4] indicates that the stress intensity factor over T ratio increases non linearly with non dimensional crack length.

c) The T-stress can explain also why dynamic critical stress intensity factor is higher than the static one according to Jayadevan et al [5].

d) Rice [6], Larsson and Carlsson [7] have shown that sign and magnitude of the T-stress substantially change the size and shape of the plane strain crack tip plastic zone. Positive or negative the T-stress increases the plastic zone size comparing with no T-stress situation. In plane strain, plastic zone is oriented along crack extension for T > 0 and in opposite sense when T <0.

d) It has been noted that in the Paris law regime, fatigue crack growth rate decreases when T increase [8].

e) Analytical and experimental studies show that the T-stress can be used as a measure of constraint ahead of the crack tip. Sumpter [9], Chao et al [10] and Hancock et al [11] have shown that the fracture toughness increases when (–T) increases.

f) It has been seen that the T-stress has an influence on crack propagation after initiation [12]. Negative T-stress values stabilise crack path. In opposite, positive T-stress value induces crack bifurcation.

Crack stabilisation is sensitive to the so-called biaxiality ratio β

$$\beta = \frac{T\sqrt{\pi a}}{K_I} \qquad (2)$$

where a is the crack length. If the value of triaxiality increases, stabilisation of crack path increases.

The concept of the T-stress as a constraint factor has been extended to notch tip stress distribution as the effective T-stress T_{ef}. The fracture toughness measured from notched specimen as the critical notch stress intensity factor has been determined using the Volumetric Method [13]. Transferability is then proposed as a $K_{\rho,c} - T_{ef,c}$ curve and established from 4 specimen types (CT, SENT, DCB and RT) made from X52 pipe steel. Discussion about crack stabilisation and crack bifurcation for fracture emanating from notches is carried out in the last section.

THE T-STRESS FOR A CRACK AND THE T_{ef}–STRESS FOR A NOTCH

Several methods have been proposed in literature to determine the T-stress for cracked specimens. The stress difference method (SDM) has been proposed by Yang et al [14]. In this method, the T-stress is evaluated from the difference between opening stress and

stress which is parallel to the crack line. To calculate the stresses, finite element method is successfully used. Other methods of T-stress calculations are presented in Refs. [15-17].

In this paper, the SDM has been employed to calculate the T-stress in a notched body because it is the most simple and widely used. The T-stress for the notch has been evaluated by experimental and numerical methods.

Numerical determination

The T-stress definition is based on the SDM as follows

$$T = \left(\sigma_{xx} - \sigma_{yy}\right)_{\theta=0}.$$ (3)

The T-stress is evaluated using finite element method and computing the difference of principal stresses along ligament for direction $\theta=0$. It should be noted that the T-stress can be evaluated in any direction (table 1).

Table 1. T-stress values according to measurement direction.

$\theta = 0$	$\theta = \pm\pi$	$\theta = \pm\pi/3$	$\theta = \pm\pi/2$	$\theta = \pm 2\pi/3$
$T = \left(\sigma_{xx} - \sigma_{yy}\right)$	$T = \sigma_{xx}$	$T = \sigma_{xx} - \sigma_{yy}/3$	$T = \sigma_{xx} - \sigma_{yy}/3$	$T = \left(\sigma_{xx} - \sigma_{yy}\right)$

It can be seen that T is not really constant as in theory (Fig. 1).
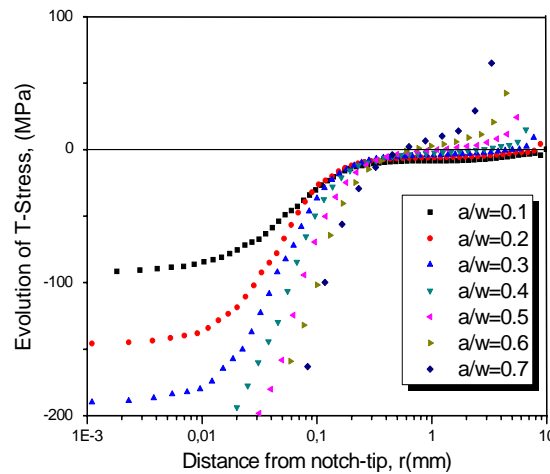
Figure 1. T-stress distribution along ligament for a roman tile specimen with large range of the notch aspect ratio [a/t = 0.1-0.7].

For short crack, distribution of the T-stress is stabilised after some distance. For long crack, T increases linearly with ligament except a region which is close to the crack tip.

205

Therefore, it is necessary to use a conventional definition of the T-stress to overcome this difficulty. Maleski et al [18] suggest representing the T-stress by the following relationship

$$T(x)=T_0 + \lambda(x/a))$$
(4)

By extrapolation $r \to 0$, they obtain T_0 value and consider this value as the acting T-stress.

Using the volumetric method [13], we have suggested defining an effective T-stress calculated as the average value of the T-stress distribution in the region corresponding to the effective distance determined (Fig. 2). The acting T stress is named T_{ef}.
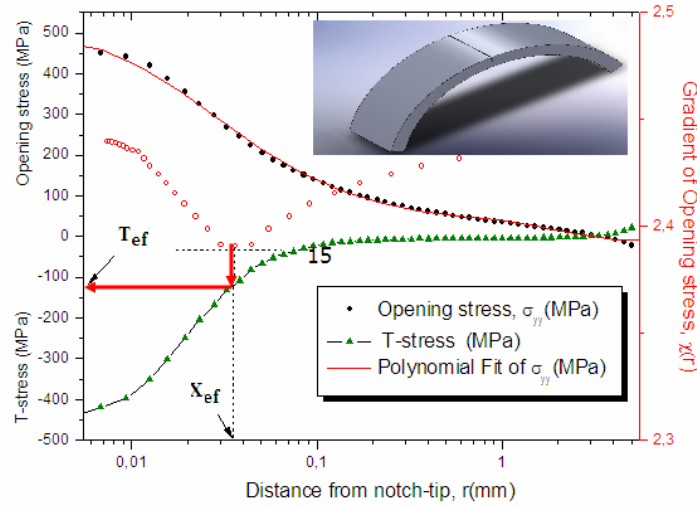
Figure 2. Definition of the T_{ef}- stress from the T-stress distribution at a distance equal the effective distance X_{ef} determined by Volumetric Method.

Experimental determination of the T-stress

This method is based on William's solution [1].The T-stress can be measured using strain gauges glued in particular directions (Fig. 3). The T-stress is measured using a rectangular rosette with the difference between the normal strains in polar coordinates after α rotation

$$
\begin{aligned}
E(\varepsilon_{rr} - \varepsilon_{\theta\theta}) = &\, A_1 r^{-1/2}(1+v)\sin\theta\left[\cos\frac{3\theta}{2}\sin 2\alpha - \sin\frac{3\theta}{2}\cos 2\alpha\right] \\
&+ 2A_2(1+v)r^0\cos 2\alpha \\
&+ A_3 r^{1/2}(1+v)\sin\theta\left[\sin\frac{\theta}{2}\cos 2\alpha - \cos\frac{\theta}{2}\cos 2\alpha\right] \\
&+ 2A_4 r^1(1+v)[\cos\theta + \cos 2\alpha - 2\sin\theta\sin 2\alpha]
\end{aligned}
$$
(5)

where E and v are Young's modulus and Poisson' ratio, respectively. In this equation, coefficient A_1 is proportional to mode I stress intensity factor K_I and A_2 is proportional to the T-stress. For three θ angles ($\theta = 0, \pm\pi, \pm 2\pi/3$) A_1 factor is eliminated from the difference $(\varepsilon_{rr} - \varepsilon_{\theta\theta})$. The angles $\theta = 0, \pm\pi$ cannot be chosen for practical reason as gauge directions. Taking the values $\theta = \pm 120°$, Eq. 5 leads to

$$\frac{E}{1+v}\left(\varepsilon_{xx} - \varepsilon_{yy}\right) \approx 2A_2 + \frac{3A_3 r^{1/2}}{4} - A_4 r. \tag{6}$$

If r is small, an approximation of Eq. 6 gives

$$\frac{E}{1+v}\left(\varepsilon_{xx} - \varepsilon_{yy}\right) \approx 2A_2. \tag{7}$$
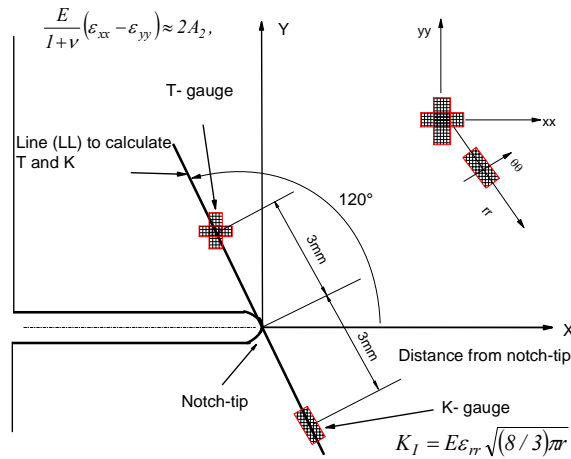
Figure 3. Positions and directions used to determine the T-stress and the notch stress intensity factor using strain gauges.

The T-stress is measured by this experimental method at a point located at 3 millimetres from the notch tip and is called $T^*_{\rho,3mm}$. When the T-stress is measured for fracture load, a subscript c is added. Computed values are generally higher than experimental values (average increase is 15%). In the following, the computed T value is called T_{ef} and keeps as results.

Material properties and specimen geometries
The material used in this study is an X52 steel meeting requirements of API 5L standard. In table 2, the mechanical properties of API X52 have been presented. E, σ_y, σ_u, A%, n, k and K_{Ic} are the Young's modulus, yield stress, ultimate stress,

207

elongation at fracture, strain hardening exponent and hardening coefficient in the Ramberg-Osgood law, the fracture toughness, respectively.

Table 2. Mechanical properties of API X52.

E, GPA	σ_y, MPa	σ_u, MPa	A, %	n	k	K_{Ic} $MPa\sqrt{m}$
210	410	528	32	0.164	876	116.6

Several specimens of 4 types, namely, CT, DCB, SENT and RT (roman tile) were extracted from a steel pipe of diameter 610 mm. Geometries of these specimens are given in Fig. 4 a, b, c and d. The specimens have a notch with a notch angle $\varphi = 0$ and a notch radius $\rho = 0.25$ mm. For each geometry, three notch aspect ratio were used (a/W= 0.2 ; 0.3 ; 0;5).
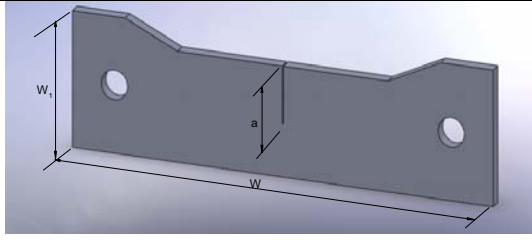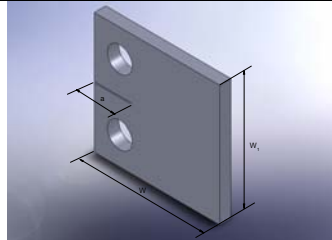
Figure 4a. SENT specimen: thickness 5.8 mm, width 58.40 mm.	Figure 4b. CT specimen: thickness 5.8 mm, width 63.80 mm, height 61 mm.
Figure 4c. DCB specimen: thickness 5.8 mm, height 45.70mm.	Figure 4d. Roman tile specimen: thickness 5.8 mm, width 40 mm, length 280 mm.
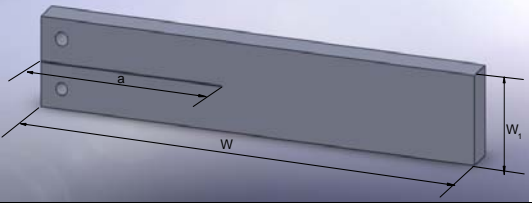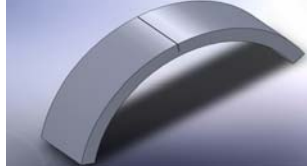
Fracture initiation is detected by acoustic emission and provides the load for crack initiation. A sudden drop in the registered signal of gauges corresponds to critical load.

Determination of the critical notch stress intensity factor
Numerical determination of the critical notch stress intensity factor was carried out through computing of the stress distribution at the notch tip for initiation and fracture

loads. Using the procedure of the Volumetric Method, the effective distance X_{ef} was extracted from the stress distribution at distance from the notch tip where the relative stress gradient is minimum value. Then, the effective stress σ_{ef} is determined through a line method: the effective stress is defined as the mean value of the stress distribution $\sigma_{yy}(r)$ over the effective distance

$$\sigma_{ef} = \frac{1}{X_{ef}} \int_0^{X_{eff}} \sigma_{yy}(r)dr .$$ (8)

The critical notch stress intensity factor $K_{\rho,c}$ is estimated as follows

$$K_{\rho,c} = \sigma_{ef,c}\sqrt{2\pi X_{ef,c}} .$$ (9)

It should be noted that notch fracture mechanics uses traditionally the line method but generally the difference with the point method is small.

The notch stress intensity factor K_ρ can be also obtained by experimental method using strain gauge (see Fig. 3) using approach proposed by Dally and Sanford [19]

$$K_\rho = E\varepsilon_{rr}\sqrt{(8/3)\pi r} .$$ (10)

The critical value of the notch stress intensity factor is then given by the following equation

$$K_{\rho,c}^{**} = E\varepsilon_{rr,c}\sqrt{(8/3)\pi \cdot 3 \cdot 10^{-3}} .$$ (11)

The strain gauge is glued at 3 millimetres from notch tip.

The $K_{\rho,c} - T_{ef,c}$ material failure curve

The $K_{\rho,c} - T_{ef,c}$ curve is built in order to create a material characteristic taking into account specimen geometry, ligament size, loading mode. To get different assessment points ($K_{\rho,c}, T_{ef,c}$), 4 different specimen geometries (CT, SENT, RT and DCB) with several notch aspect ratio were tested.

An example of $K_{\rho,c} - T_{ef,c}$ diagram is given for the case of roman tile specimens with a/t=0.4; 0.5; 0.6 (Fig. 5). Here, t is the specimen thickness. It can be seen that the critical notch stress intensity factor is a decreasing function of the $T_{ef,c}$-stress. The value of $T_{ef,c}$ decreases with the notch aspect ratio of 20 % when a/t increases from a/t =0.4 to a/t = 0.6.
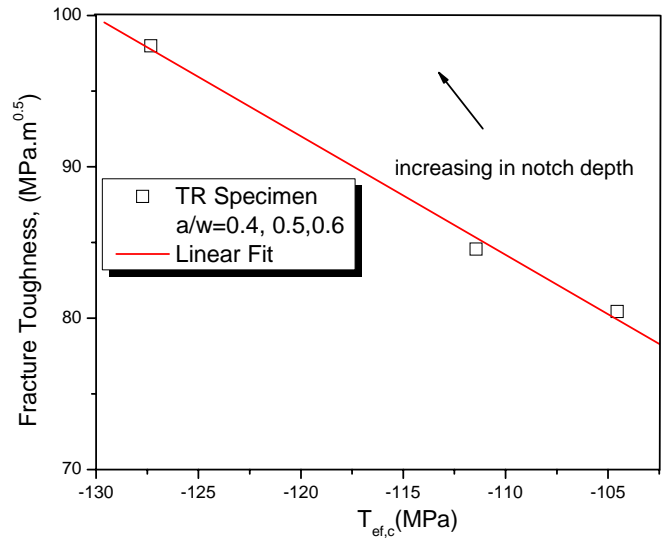
Figure 5. $K_{\rho,c} - T_{ef,c}$ diagram for the case of roman tile specimens and for notch aspect ratio $a/t = 0.4$; 0.5; 0.6.

Computing the stress distribution ahead of the notch tip leads to the following results. The parameter A_3 is practically equal to zero until a/t= 0.3. For larger value of a/t, negative values of A_3 increase, and the approximation given by Eq. 7 is no longer valid. In this case, fracture toughness transferability needs two parameters (T and A_3) for values of a/t >0.3.

All experimental assessment points $(K_{\rho,c}, T_{ef,c})$ for 4 specimen types are summarized in Fig. 6.
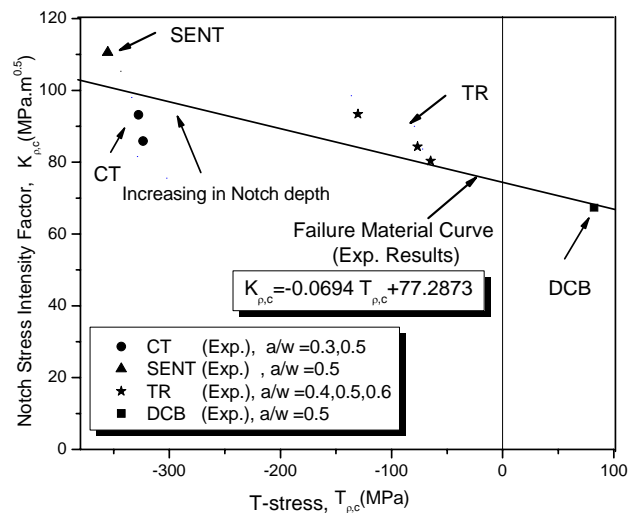
Figure 6. $K_{\rho,c} - T_{ef,c}$ material master curve for X52 pipe steel.

These results allow drawing a material failure curve called also material master curve. A linear relationship was found

$$K_{\rho,c} = aT_{ef,c} + b \qquad (12)$$

with a and b material constants which are *a* = -0.069 and *b* =77.28 for X52 steel. The master curve is a way to take into account the constraint effect on the fracture toughness and is associated with the driving force diagram in order to establish fracture conditions.

We have analyzed the measured fracture toughness for different precracked specimen geometries published in 4 references [11, 20-22]. Results are presented in table 3 which includes our results obtained for notched specimens. All results are coherent and indicate the following: tensile specimens have always higher fracture toughness than bending specimens. This is due to high negative T-stress values for tensile specimens and consequently lower constraint.

Table 3. Comparison of the fracture toughness for different specimen geometries.

references	specimens	Fracture toughness
[11] ASTM 719 Grade A steel	CT(a/W=0.5), SENB (a/W=0.5)	SENB>CT
[19] ASI 1405-180	SENT(a/W=0.5) ; SENB(a/W=0.5) DENT (a/W=0.5), CCT (a/W=0.5), CT (a/W=0.6),	DENT > CCT>SENT >SENB ~ CT
[20] FYO HY 100 Alloy steel	SENT (a/W=0.65), SENB(a/W=0.61), DENT (a/W=0.61),	SENT>SENB> DENT
[21] PMMA	SENT (a/W=0.3-0.6), CT (a/W=0.3-0.7), DCB (a/W=0.1-0.7),	CT~DCB>SENT
Present results	SENT (a/W=0.5), CT (a/W=0.1;0.3; 0.5), DCB (a/W=0.5), TR (a/t=0.4 ; 0.5 ; 0.6)	SENT> CT>RT> DCB

Crack stabilisation or bifurcation according to the T_{ef} -stress
The $T_{ef,c}$ range for each specimen type is reported in table 4 (σ_y is the yield stress).

Table 4. $T_{ef,c}$ range for different specimen configuration.

Specimen	SENT	CT	RT	DCB
$T_{ef,c}$ range	-0,74 σ_y ; -0.80 σ_y	- 0.53 σ_y ; -0.67 σ_y	- 0.25 σ_y ; -0.30 σ_y	0.19 σ_y ; 0.21 σ_y

Tensile specimens have higher negative $T_{ef,c}$ range in comparison with bending specimen. It means that constraint is less for tensile specimen. The DCB specimens exhibit particular positive $T_{ef,c}$-stress values. These positive $T_{ef,c}$-stress values have some influence on stability of crack propagation. The SENT and CT specimens have a high negative value of the $T_{ef,c}$-stress. For these specimens, crack extension is observed along x direction, i.e. perpendicular to the principal tensile stress. This can be clearly seen in Fig. 7a and b.

Figure 7a. Stable crack extension in SENT specimen. $T_{ef,c}$ = -348 MPa	Figure 7b. Stable crack extension in CT specimen. $T_{ef,c}$ = -328 MPa
Figure 7c. Crack bifurcation in DCB specimen. $T_{ef,c}$ = + 78 MPa.	Figure 7 d. Stable crack extension in TR. $T_{ef,c}$ = - 111 MPa.
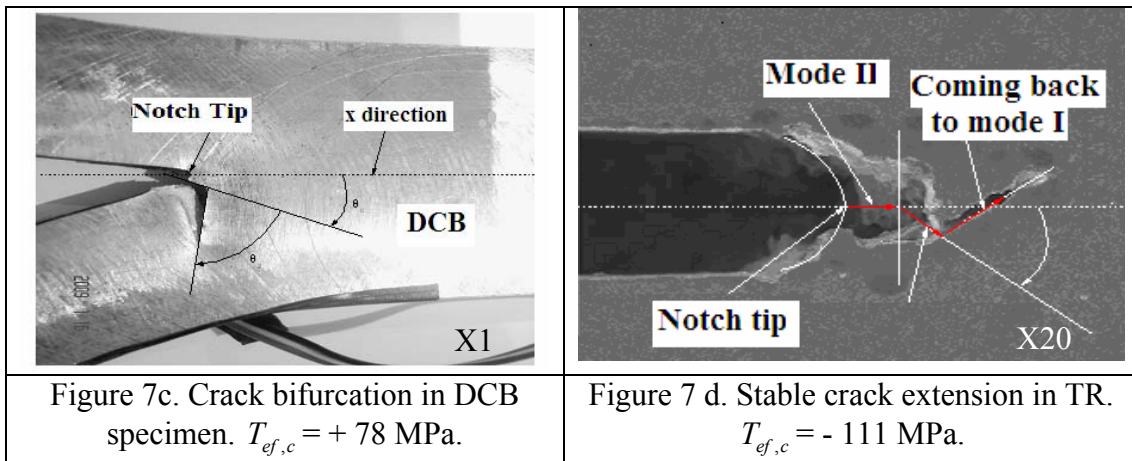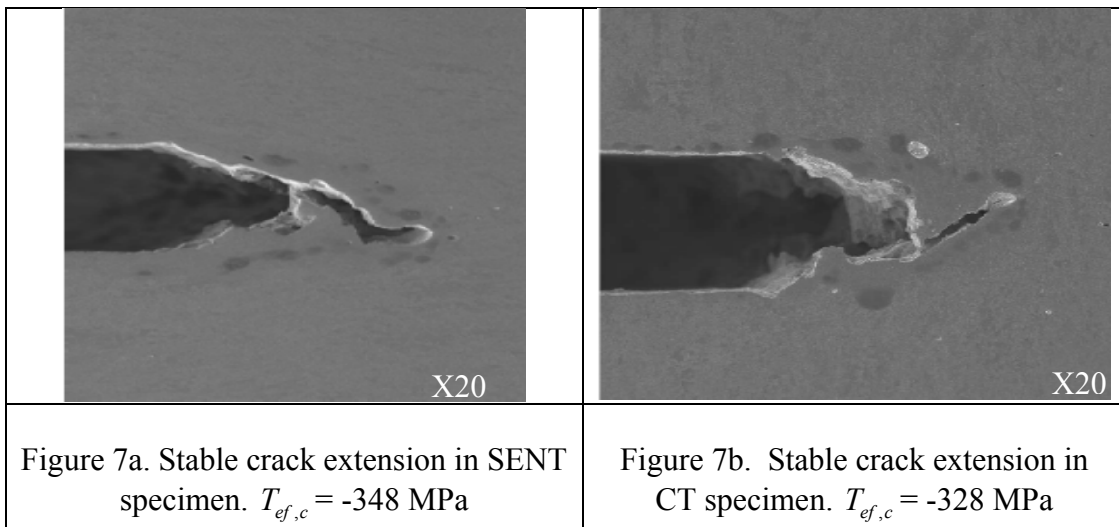
Crack bifurcation appears after initiation in DCB specimens, this well-known phenomenon is an attribute of positive T-stress [10]. In order to prevent crack bifurcation, it is recommended to use the tapered DCB specimen. In this case, we return to a specimen with a negative $T_{ef,c}$ value, and for this reason the crack extension is stable in x direction.

Fracture occurs in X52 Pipe steel by ductile failure. The failure mechanism is governed by the following sequences: voids nucleation, voids growth and coalescence. Voids growth is sensitive to stress triaxiality, and growth occurs mainly in direction according to principal tensile stress. Due to hard particles inside the voids (these particles promote voids nucleation by stress concentration), voids cannot be closed by compressive (negative) T-stress and crack extension is then stable in notch direction according to scheme in Fig. 7a. If the T-stress is positive and higher than opening stress at some distance ahead of the notch tip, void extension then occurs in x direction which is corresponding to the maximum $T_{ef,c}$-stress direction. In this case, crack extension is made by bifurcation according to Fig. 7c.

| Figure 7a | Figure 7b | Figure 7c |
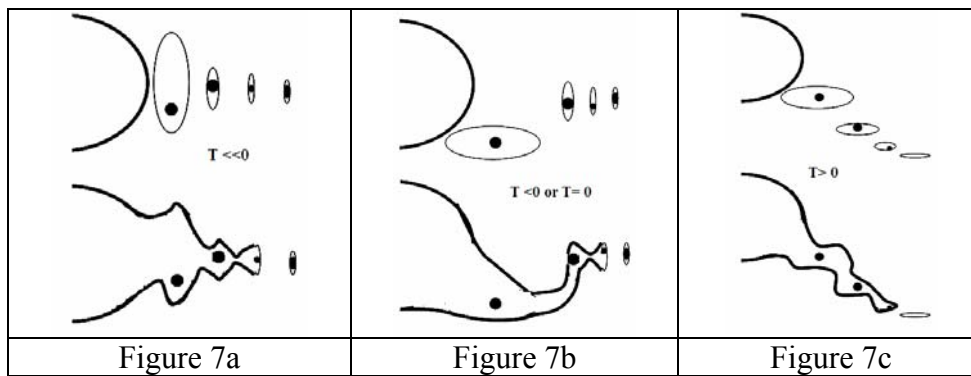
Figure 7. Proposed mechanisms for ductile crack extension under negative or positive $T_{ef,c}$-stress.

CONCLUSIONS

The concept of the T-stress ahead of the crack tip has been adopted for notch fracture mechanics according to the idea that the crack is a special case of notches.

Similar difficulties appear for determination of the T-stress for cracks and the $T_{ef,c}$-stress for notches, namely, the T-stress distribution is not constant along ligament of the specimen. To overcome this difficulty, it has been proposed to use the effective T-stress which is the average value of the T-stress distribution at the effective distance provided by Volumetric Method. The obtained values are close to the extrapolated value of T_0 suggested by Malewski et al [18].

A large range of $T_{ef,c}$-stress values is investigated for different specimen configurations. For SENT, CT, RT and DCB specimens made from X52 pipe steel, positive and negative values are obtained: the $T_{ef,c}$-stress range is varied from $-0.8\,\sigma_y$ to $0.1\,\sigma_y$. A gap of the $T_{ef,c}$-stress values exists between CT and RT specimens.

The obtained results allow constructing a material master curve $K_{\rho,c} = f\left(T_{ef,c}\right)$, where the notch fracture toughness is a linear decreasing function of the $T_{ef,c}$ -stress.

It has been noted that negative $T_{ef,c}$ -stress value promotes crack extension and positive one promotes crack bifurcation. A mechanism involving influence of the $T_{ef,c}$ - stress on void growth for ductile failure is proposed.

REFERENCES

1. Williams, J.G. and Ewing, P.D. (1972) *Int. J. Fract.* **8**, 416-441.
2. Eisele, U. and Roos, E. (1990) *Nuclear Engineering and Design* **130**, 237-247.
3. Matvienko, Yu. G. (2008) In: *17th European Conference on Fracture*, September 2-5, Brno, Czech Republic.
4. Sherry, A.H., France, C.C. and Goldthorpe, M.R. (1995) *Fatigue and Fracture of Engineering Materials and Structures* **18**, 141-155.
5. Jajadevan, K.R., Narasimhan, R., Ramamurthy,T.S. and Dattaguru, B. (2001) *Int. J. Fract.* **38**, 4987-5005.
6. Rice, J.R. (1974) *J. Mech. Phys. Solids* **22**, 17-26.
7. Larsson, S.G and Carlsson, A.J. (1973) *J. Mech. Phys. Solids* **21**, 263-278.
8. Kabiri, M.R. (2003) Thèse Ecole des Mines de Paris, France.
9. Sumpter, J.D.S. (1993). In: *ASTM STP 1171*, pp. 492-502, Hackett, E. M., Schwalbe, K.-H. and Dodds, R.H. (Eds.), American Society for Testing and Materials, Philadelphia.
10. Chao,Y.J., Lam, P.S. and Zhang, L. (1998) *Theoretical and Applied Fracture Mechanics* **30**, 75-86.
11. Hancock, J.W., Reuter, W.G. and Parks, D.M. (1993). In: *ASTM STP 1171*, pp. 21-40, Hackett, E. M., Schwalbe, K.-H. and Dodds, R.H. (Eds.), American Society for Testing and Materials, Philadelphia.
12. Leevers, P.S. and Radon, J.C. (1982) *Int. J. Fract.* **19**, 311-325.
13. Pluvinage, G. (2003) *Fracture and Fatigue Emanating from Stress Concentrators*, Kluwer Academic Publishers, Dordrecht/Boston/London.
14. Yang, B. and Ravichandar, K. (1999) *Engng Fract. Mech.* **64**, 589-605.
15. Chao, Y.J., Liu, S. and Broviak, B.J. (2001) *Experimental Mechanics* **41**, 232-241.
16. Ayatolahi, M.R, Pavier, M.J. and Smith, D.J. (2002) *Int. J. Fract.* **117**, 159-174.
17. Wang X. (2003) *Engng Fract. Mech.* **70**, 731-756.
18. Maleski, M.J., Kirigulige, M.S. and Tippur, H.V. (2004) *Society for Experimental Mechanic*s **44**(5), October.
19. Dally, J.W. and Sanford, R.J. (1987) *Experimental mechanics* **49**, 381-388.
20. Wu, S., Mai, Y.W. and Cotterell, B. (1995) *J. Mech. Phys. Solids* **43**, 793-810.
21. Joyce, J.A, Hackett, E.M. and Roe, C. (1992) *NUREG CR-5879 US Nuclear Regulatory Commission*.
22. Liu, S. and Chao, Y.J. (2003) *Int. J. Fract.* **124**, 113-117.